Large amplification of the sensitivity of symmetric-response magnetic tunnel junctions with a high gain flux concentrator

Samuel Manceau, Thomas Brun, Johanna Fischer, Clarisse Ducruet, Philippe Sabon, Claude Cavoit, Guillaume Jannet, Jean-Louis Pinçon, Ioan Lucian Prejbeanu, Matthieu Kretzschmar, et al.

RESEARCH ARTICLE | AUGUST 22 2023

Large amplification of the sensitivity of symmetric-response magnetic tunnel junctions with a high gain flux concentrator

Samuel Manceau ; Thomas Brun ; Johanna Fischer ; Clarisse Ducruet; Philippe Sabon; Claude Cavoit; Guillaume Jannet ; Jean-Louis Pinçon; Ioan Lucian Prejbeanu ; Matthieu Kretzschmar ; Claire Baraduc

Appl. Phys. Lett. 123, 082405 (2023)
https://doi.org/10.1063/5.0160544

Applied Physics Letters ARTICLE pubs.aip.org/aip/apl

Large amplification of the sensitivity of symmetric-response magnetic tunnel junctions with a high gain flux concentrator

Cite as: Appl. Phys. Lett. **123**, 082405 (2023); doi: 10.1063/5.0160544
Submitted: 2 June 2023 · Accepted: 27 July 2023 ·
Published Online: 22 August 2023

Samuel Manceau,[1,2] Thomas Brun,[1,2] Johanna Fischer,[1] Clarisse Ducruet,[3] Philippe Sabon,[1] Claude Cavoit,[2] Guillaume Jannet,[2] Jean-Louis Pinçon,[2] Ioan Lucian Prejbeanu,[1] Matthieu Kretzschmar,[2] and Claire Baraduc[1,a)]

AFFILIATIONS

[1]University Grenoble Alpes, CEA, CNRS, Grenoble INP, SPINTEC, 17, Avenue des Martyrs, 38054 Grenoble, France
[2]LPC2E, UMR7328 CNRS and Université d'Orléans, 3 Avenue de la Recherche Scientifique, 45071 Orléans, France
[3]Crocus Technology, 3 Avenue Doyen Louis Weil, 38000 Grenoble, France

[a)]Author to whom correspondence should be addressed: claire.baraduc@cea.fr

ABSTRACT

Miniaturized, ultra-sensitive and easily integrable magnetometers are needed for many applications like space exploration or medical survey. In this study, we combine innovative magnetic tunnel junctions having a symmetric resistance-field (R–H) response with a high gain flux concentrator. In our junctions, the magnetization of the free layer (FL) is stabilized in an anti-parallel configuration with respect to that of the reference layer. This configuration is achieved by using a soft exchange pinning of the FL. We precisely adjust the exchange field value with a dusting layer of ruthenium used to weakly decouple the magnetization of the FL from the local moments of the antiferromagnet. In order to improve the junction's sensitivity, we study the influence of the exchange field value and of the shape anisotropy on the even-function R–H response. In particular, we compare circular junctions with elliptic or rectangular junctions of various aspect ratios and orientations. We find that the sensitivity of the junctions increases when reducing the soft-pinning exchange field and by using junctions with an elongated shape in the direction of the applied field. Finally, we were able to further increase the sensitivity by a factor 440 due to a flux concentrator placed around the junction by electrochemical deposition of NiFe. Its design is optimized (elongated shape, 5–7 μm thickness and 10 μm air-gap) in order to obtain this very high gain. The complete sensor system composed of these magnetic tunnel junctions and the flux concentrator allows to reach sensitivities larger than 1000%/mT.

To detect ultra-low magnetic fields, magnetic flux sensors such as SQUIDs, search-coils, or flux-gates are usually considered as the best options. However, these solutions are large and heavy, which limits considerably their use in environment with limited available space and weight, as, for example, onboard small satellites envisioned to monitor the solar wind and the near Earth's environment. Moreover, the integration of ultra-sensitive sensors within small systems is required for various applications, particularly for biosensors like lab-on-chip or a wearable device for health monitoring. In order to decrease the detection limit of integrable sensors, magnetoresistive sensors based on spin valves or magnetic tunnel junctions (MTJs) have emerged.[1,2] High tunnel magnetoresistance (TMR) values combined with a low noise level have enabled low footprint magnetometers[3] with increased performances. Further improvements can be achieved by using an array of inter-connected MTJs to reduce the 1/f noise or by adding magnetic flux concentrators[4] to increase the sensitivity. In a recent work, sub-pT detectivity at low frequencies was achieved[5] by combining advantageously these two approaches.

Hitherto, research has been focused on sensors with a linear response of the electric resistance to the magnetic field. Such MTJ-based sensors require several steps of annealing under magnetic field to set the free layer (FL) and reference magnetizations perpendicular to each other.[6] Moreover, in order to obtain a full Wheatstone bridge configuration, local annealing is needed to set half of the reference magnetizations in one direction and the other half in the opposite orientation. In this study, we develop a magnetic sensor using MTJs that have a symmetric response (SR) instead of a linear response based on the concept that we proposed previously.[7] SR sensors, having, namely,

the same resistance for positive and negative field, present some advantages. For example, they can be used as encoders to detect the position of a moving part with a better spatial resolution compared with a linear sensor; indeed, for the same displacement of a magnet in front of the sensor, a SR sensor shows two oscillations, while a linear sensor shows only one.[8] The SR sensors have also been proposed with a modulation scheme to reduce 1/f noise,[7,9] but a recent study[8] has shown that the low frequency magnetic noise is transferred at the modulation frequency, resulting in a limited benefit. SR sensors remain interesting since their fabrication requires only a single field-annealing step. In particular, the same junction presents a response curve with either a positive or a negative slope depending of the chosen working point, which makes SR-MTJs good candidates for integration in a full Wheatstone bridge.

In this work, we experimentally demonstrate the combination of SR-MTJs with a high-gain magnetic flux concentrator to further increase the sensitivity. For the development of our micrometer-sized junctions, we face the usual trade-off between the need of a uniform (macrospin) magnetization in the free layer and the ability of the magnetization to freely rotate under field. We solve this issue by using the soft-pinning technique described in the literature,[10,11] which consists in pinning the free layer magnetization by weak exchange coupling with an antiferromagnet. Herein, we investigate the impact of three main features of our sensors on their sensitivity: the value of the soft-pinning exchange field, the junction geometry, and the properties of a high gain flux concentrator.

The SR-MTJs studied in this work are composed of the following magnetic multilayer grown by conventional DC magnetron sputtering on a CuN buffer: IrMn/CoFe/Ru/CoFeB/MgO/CoFeB/Ta/NiFe/Ru/IrMn/Ru. The reference layer (RL) is a standard synthetic antiferromagnetic (SAF) multilayer exchange biased with an IrMn layer. The MgO tunnel barrier is obtained by successive deposition of Mg layers followed by natural oxidation under partial oxygen pressure and has a resistance per area product (RA) of about 5 kΩ μm^2. For the free layer (FL), we chose to use a bilayer of CoFeB and NiFe separated by a dusting layer of Ta (<0.5 nm) acting as a texture breaking layer and as a boron getter. The CoFeB layer in contact with the tunnel barrier favors a high tunnel magnetoresistance ratio (TMR), thanks to the high spin polarization of the electrons. The addition of 5 nm of NiFe increases the sensitivity of the free layer to the external magnetic field because of its low saturation magnetization. The soft-pinning of the FL is obtained by exchange bias with an IrMn antiferromagnetic layer via a ruthenium dusting spacer of ultrathin thickness X < 1 nm. The higher the ruthenium thickness, the less coupled is the free layer and the weaker is the exchange bias field.[10,12] Contrary to this technique, Nakatani and coworkers[8] used orange-peel coupling to softly pin a CoFeBTa free layer of an inverted stack SR-MTJ. After deposition, small samples dedicated to magnetic characterization are field-annealed at a temperature of 310 °C. Annealing under these conditions allows the crystallization of the tunnel barrier and its adjacent layers, as well as the pinning of the magnetizations of the reference and free layers by exchange coupling with the IrMn antiferromagnetic layers. The magnetic properties of the stack are measured with a vibrating sample magnetometer (VSM) along the planar easy and hard magnetization axes. The easy axis hysteresis loop allows, namely, to evaluate the pinning of the synthetic antiferromagnet and to measure the exchange bias field (H_{ex}) of the soft-pinned layer by the shift of the hysteresis cycle. In particular, we evidenced the decrease in H_{ex} from 15 to 0.63 mT with the increase in the nominal thickness of the Ru layer from X = 0 to 0.55 nm. The magnetocrystalline anisotropy of the free layer (H_k = 5.6 mT) is extracted from the measurement of the saturation field in the hard magnetic axis direction, which is equal to the sum of the exchange bias and anisotropy fields.

Junctions are defined by optical lithography. The pillars, protected by a hard mask of Ta, are etched by ion beam etching under oblique incidence down to the bottom layer of IrMn. The bottom electrode is then patterned by lithography and etching, and the junction is encapsulated in a spin-on-glass planarizing resist, before opening the top contact by reactive ion etching. After the microfabrication, the wafer is annealed under magnetic field to cure the defects induced by the etching and to ensure the correct orientation of the magnetizations. After annealing, the magnetization of the free layer is oriented in the same direction as the magnetization of the pinned layer (i.e., bottom layer of the SAF). At zero field, the junction is in the antiparallel state: the magnetization of the reference layer (upper layer of the SAF) and that of the free layer are aligned along the direction of easy magnetization (noted y) but in opposite orientations (see the inset of Fig. 1). Figure 1 shows a schematic view of these layers and the response of a circular junction of 4 μm nominal diameter under fields applied along the easy and hard axis. Sweeping the field along the easy axis, we observe a resistance plateau in positive (respectively, negative) fields corresponding to the parallel (respectively, antiparallel) state of the junction. The transitions between the two states are sharp, and the hysteresis cycle is shifted by the value of the exchange field of the junction due to soft-pinning, here equal to H_{ex} = 2.01 mT. The TMR measured under a bias voltage of 100 mV is equal to 130%.

In order to obtain a symmetric response sensor, the external magnetic field is applied along the hard axis (x-axis): the response curve is smooth, without hysteresis and quasi-symmetric. These three characteristics result from the used soft-pinning technique. The response curve is significantly improved compared to our previous work[7] using the combined effect of magnetocrystalline and shape

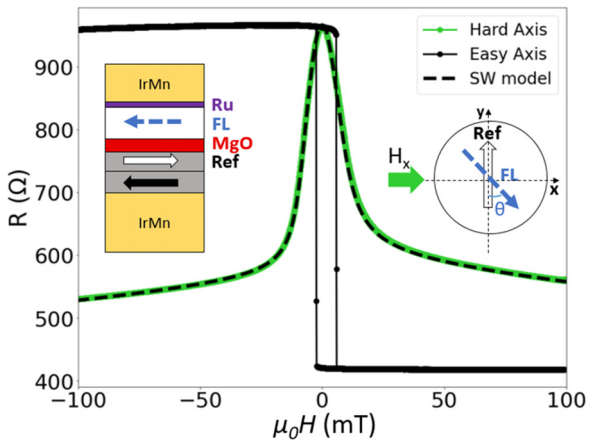

FIG. 1. Resistance vs magnetic field of a 4 μm diameter circular junction with 0.3 nm Ru spacer. Magnetic field is applied along easy (black) and hard (green) axes. The dashed line is the fit using the Stoner Wohlfarth model with $\mu_0 H_{ex}$ = 2.6 mT, $\mu_0 H_k$ = 6.6 mT, $\mu_0 H_R$ = 450 mT, and δ = 4.05°. Insets: side view (left) and top view (right) of the magnetic tunnel junction.

anisotropy. The hard axis response corresponds to the coherent rotation of the FL magnetization from the anti-parallel state, at zero field, to the $\pm 90^\circ$ state, at saturation field. For a perfectly pinned reference magnetization, the junction reaches the resistance corresponding to the orthogonal configuration of magnetizations. This state corresponds to the average of the conductance in the parallel and antiparallel states, i.e., a resistance equal to

$$R_\perp = R_P \frac{2(1+TMR)}{2+TMR}, \tag{1}$$

where R_P is the resistance in the parallel state, and $TMR = (R_{AP} - R_P)/R_P$ is the magnetoresistance ratio. It can be seen that the resistance measured along the hard axis at large fields is lower than $R_\perp$, which can be explained by a slight rotation of the reference magnetization toward the applied field.

The symmetric response curve can be fitted by a Stoner–Wohlfarth model taking into account the magnetocrystalline anisotropy and shape anisotropy energy (for non-circular junctions), the exchange coupling energy and the Zeeman energy. The orientation of the free-layer magnetization with respect to the easy axis, defined by the angle θ, is expressed as a function of the external ($h = H/M_s$), anistropy ($h_k = H_k/M_s$), and exchange ($h_{ex} = H_{ex}/M_s$) fields, normalized by the saturation magnetization M_s,

$$h = h_k \sin\theta + h_{ex} \tan\theta. \tag{2}$$

The reference layer is also considered to rotate with a rotation angle θ_R with respect to its initial orientation, according to the equation $\tan\theta_R = H/H_R$, where H_R is the saturation field of the reference layer. The conductance G of the junction can then be calculated using the standard formula,

$$G = \frac{G_P + G_{AP}}{2} + \frac{G_P - G_{AP}}{2}\cos\varphi, \tag{3}$$

where $\varphi = \pi - (\theta + \theta_R)$ is the angle between the magnetizations of the FL and reference layer. It is also possible to account for a possible misalignment (δ) of the external field with respect to the hard axis, which is responsible for the slight deviation from symmetry observed in Fig. 1. This model allows a very satisfactory fit of the measured curve (see Fig. 1). The parameters H_k and H_R are extracted from the VSM measurements, and H_{ex} is defined by the shift of the easy axis magnetoresistance cycle. Nevertheless, in order to obtain a good fit of the experimental curve, the saturation field of the reference must be chosen significantly lower (450 mT) than the one measured by magnetometry (700 mT); this decrease in the saturation field is probably explained by a degradation of the SAF coupling by the microfabrication process.

The sensitivity of the junction is defined by the maximum slope of the magnetoresistance curve $R(H)$, normalized by the resistance at this operating point. It is equal to 3.6%/mT for the junction in Fig. 1. This sensitivity depends on the TMR but mostly on the anisotropy and exchange fields. To determine the soft-pinning value that optimizes the sensitivity, we compared several stacks with various Ru spacer thickness: X = 0, 0.15, 0.3, and 0.55 nm. Since the TMR ratio varies slightly from one stack to another, the saturation resistance related to $R_\perp$ also varies. To simplify the comparison of the different samples, we choose to present the results using the normalized conductance $(G - G_{\min})/\Delta G$, where $G_{\min} = G_{AP}$ is the minimum conductance (in the antiparallel state) and $\Delta G = G_P - G_{AP}$. Indeed, for orthogonal magnetizations, the normalized conductance is equal to 0.5, independently of the TMR. The measured normalized conductance curves as a function of the applied magnetic field are shown in Fig. 2 for different soft-pinning values. For these measurements, the orientation of the external field was carefully adjusted to avoid any misalignment and any subsequent dissymmetry in the response curves. We observe that the sensitivity (related to the slope of the conductance curve) increases as the exchange field H_{ex} decreases. The highest sensitivity (4.1%/mT) is obtained for the sample with the lowest soft-pinning. Nevertheless, a slight hysteresis is observed on this curve. For our set of samples, the best sensitivity with negligible hysteresis (<0.21 mT at working point) is 3.6%/mT obtained for $H_{ex} = 2.51$ mT (X = 0.3 nm).

So far, we have considered circular junctions for which the only source of anisotropy is the growth and annealing of the materials. We are now interested in the influence of the junction shape on the measured sensitivity: we consider ellipses and rectangles of 0.8, 2, or 4 μm wide and 4, 10, 20, or 25 μm long, elongated either along the y- or x-axis (Fig. 3 inset). In the case of an elongation along the y-axis, the shape anisotropy adds to the magnetocrystalline anisotropy and reinforces the effect of soft-pinning by increasing the stabilization of the magnetization along the y-axis at zero field. For an elongation along the x-axis, the shape anisotropy reduces the magnetization stabilization. The sensitivity values shown in Fig. 3 are the averages of measurements performed on several junctions of the same shape. Each shape is associated with a shape anisotropy field: $H_{k,shape} = M_s(N_x - N_y)$, where N_x and N_y are the demagnetizing coefficients. With this definition, $H_{k,shape} > 0$ when the shape is elongated along y and $H_{k,shape} < 0$ when it is elongated along x. Figure 3 shows the measured sensitivities for each shape as a function of the shape anisotropy field calculated from the nominal dimensions. The formulas used to calculate the demagnetizing coefficients are exact for rectangular parallelepipeds[13] and approximate for elliptical junctions.[14] Figure 3 shows

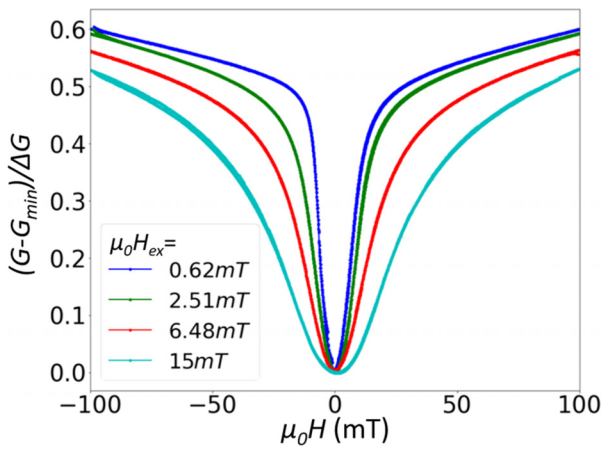

FIG. 2. Normalized conductance measured under 100 mV voltage bias, as a function of magnetic field applied along the hard axis (x-axis) for several 4 μm diameter circular junctions with decreasing values of free layer exchange field. The 15 mT exchange field corresponds to a direct contact of the free layer with the antiferromagnet (no Ru spacer).

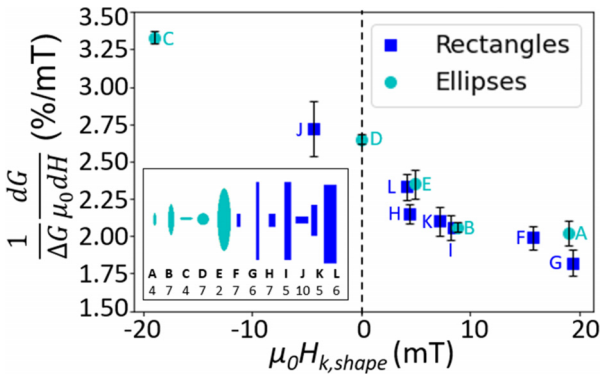

FIG. 3. Average normalized sensitivity measured on nominally identical junctions of different shapes with $\mu_0 H_{ex} = 4.75$ mT as a function of the shape anisotropy field. Squares and circles represent rectangular and elliptical junctions, respectively. The shape type is indicated close to each data point. In the inset, we precise the number of samples measured. The error bar corresponds to the standard deviation. Shapes elongated along y (x) correspond to $H_{k,shape} > 0$ (<0) and disks correspond to $H_{k,shape} = 0$. The largest values of $H_{k,shape}$ are obtained for the narrowest shapes and may be overestimated by about 3.5 mT due to lithography errors.

that the sensitivity decreases when the shape anisotropy strengthens the effect of soft-pinning ($H_{k,shape} > 0$). On the contrary, our results show that it is possible to increase the sensitivity when the shape is elongated along the axis of the applied field ($H_{k,shape} < 0$). However, large negative shape anisotropy results in a hysteretic response curve. Hence, we expect that the optimum design is an ellipse with a negative $H_{k,shape}$ that compensates for the magnetocrystalline anisotropy. Thus, changing the shape provides an additional degree of freedom to improve the sensor sensitivity. Furthermore, material engineering could help to enhance TMR and thus sensitivity, e.g., by using a nanometric insert at the MgO interface or by changing the material of the texture breaking layer (W instead of Ta) to allow for a higher annealing temperature.

Finally, we demonstrate a large increase in the sensitivity of our SR-MTJs by using a flux concentrator (FC). In contrast to previously published results, in which the gain of the concentrator is of the order of 10–100,[5,15–17] we obtain a much larger gain of 440. A gain of this order of magnitude has so far only been observed for nested flux concentrators.[18,19] The specificity of our concentrator, shown in Fig. 4, lies in its elongated shape, a very narrow air-gap (10 μm), and its large thickness of 5–7 μm. The narrowness of the air-gap requires careful repositioning during the lithography step to center the junction in the air-gap. The flux concentrator is grown by electrochemical deposition of $Ni_{80}Fe_{20}$ on a 100 mm wafer within a mold of thick patterned resist. The deposition of Ni and Fe is performed under a direct current in a solution of nickel and iron salts. The composition of the deposited material is very sensitive to the current density used.[20] In addition, mechanical strain may induce magnetostriction effects resulting in out-of-plane anisotropy in thick layers, which compromises the FC operation.[21,22] We obtain the desired stoichiometry and in-plane anisotropy via a precise control of the current density. The magnetization cycle of the FC is measured with VSM. The saturation field value of the FC (0.9 mT) corresponds the largest field that can be amplified by the FC. We notice also a slight hysteresis of about 0.1 mT; for optimal operation, further reduction of the material strain is needed in

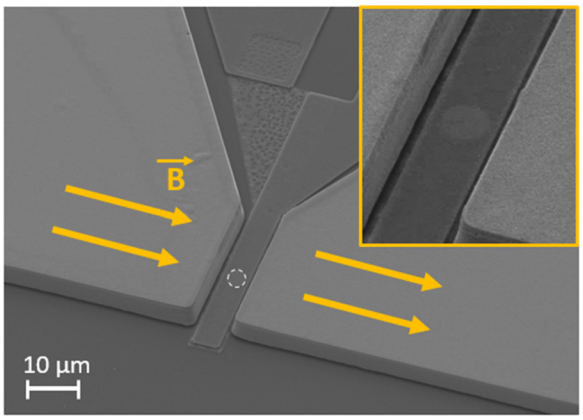

FIG. 4. Scanning electron microscope image of the flux concentrator with a circular junction within the air-gap. Inset: zoom on the junction in the air-gap.

order to suppress it. Figure 4 shows a scanning electron microscopy image of the flux concentrator's air-gap with a circular junction placed in the center: the surface of the flux concentrator is homogeneous with almost sharp edges.

The gain of the flux concentrator is estimated by comparing the measured response of the junction with and without FC. These two measurements are shown in Fig. 5: the FC produces a strong narrowing of the response curve around low fields, which is the evidence for its high gain. Furthermore, the FC allows to select the component of the external field aligned with it, which corrects any misalignment of the magnetic field. Indeed, we observe that the response curve with FC is well symmetrical. The gain is estimated by two methods: first, by calculating the ratio between the maximal slopes of the response curves with and without FC; second, by multiplying the field scale of the response curve with FC by the estimated gain until the obtained curve

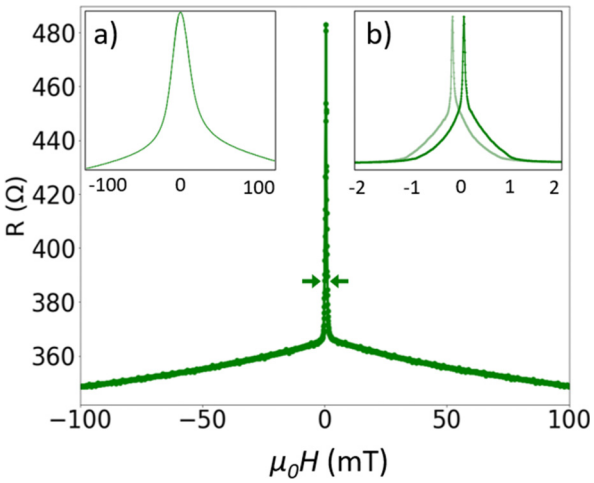

FIG. 5. Response curve of a circular junction with $\mu_0 H_{ex} = 4.75$ mT, before (a) and after the deposition of the flux concentrator. The response curve's slope is much steeper (corresponding to a sensitivity of 543%/mT) due to the high field amplification. A zoom of this curve is shown in (b) for increasing (dark) and decreasing (light) magnetic field sweep.

superimposes the response curve without FC. In the case of the responses shown in Fig. 5, the estimated gain is 440. Using this flux concentrator on our current best junctions would lead to an improvement of the sensitivity from 3.6 to 1580%/mT.

To conclude, we have fabricated junctions with symmetric response containing a free layer stabilized by a weak exchange coupling with an antiferromagnetic layer. This soft-pinning is obtained by decoupling the free layer from the antiferromagnet through a dusting layer of ruthenium. The symmetric response is obtained by applying the magnetic field perpendicular to the exchange field. A Stoner–Wohlfarth model fits the experimental curves with a very good agreement. Our measurements show that it is possible to increase the sensitivity of the junction by reducing the exchange field of the soft-pinning and by using junctions with an elongated shape in the direction of the applied field. Moreover, the use of a high gain flux concentrator (×440) allows to reach sensitivities higher than 1000%/mT. These results are promising for the future integration of ultra-sensitive sensors within small systems required for various applications, particularly for magnetometers embarked on small satellites.

This work was supported by the CNES R&T program and the ANR-22-CE42-0020 project MAROT and was partly supported by the French RENATECH network.

AUTHOR DECLARATIONS

Conflict of Interest

The authors have no conflicts to disclose.

Author Contributions

Samuel Manceau: Formal analysis (equal); Investigation (equal). **Matthieu Kretzschmar:** Funding acquisition (equal); Supervision (equal); Writing – review & editing (equal). **Claire Baraduc:** Formal analysis (equal); Funding acquisition (equal); Project administration (equal); Supervision (equal); Writing – original draft (lead); Writing – review & editing (equal). **Thomas Brun:** Formal analysis (equal); Investigation (equal); Visualization (equal); Writing – review & editing (equal). **Johanna Fischer:** Writing – review & editing (equal). **Clarisse Ducruet:** Resources (lead). **Philippe Sabon:** Methodology (lead). **Claude Cavoit:** Conceptualization (lead). **Guillaume Jannet:** Funding acquisition (equal); Project administration (lead). **Jean-Louis Pinçon:** Conceptualization (supporting). **Ioan Lucian Prejbeanu:** Writing – review & editing (equal).

DATA AVAILABILITY

The data that support the findings of this study are available from the corresponding author upon reasonable request.

REFERENCES

[1]P. P. Freitas, R. Ferreira, S. Cardoso, and F. Cardoso, "Magnetoresistive sensors," J. Phys. **19**(16), 165221 (2007).
[2]C. Zheng, K. Zhu, S. Cardoso de Freitas, J. Y. Chang, J. E. Davies, P. Eames, P. P. Freitas, O. Kazakova, C. Kim, C. W. Leung, S. H. Liou, A. Ognev, S. N. Piramanayagam, P. Ripka, A. Samardak, K. H. Shin, S. Y. Tong, M. J. Tung, S. X. Wang, S. S. Xue, X. L. Yin, and P. W. T. Pong, "Magnetoresistive sensor development roadmap (non-recording applications)," IEEE Trans. Magn. **55**(4), 1–30 (2019).
[3]F. Matos, R. Macedo, P. P. Freitas, and S. Cardoso, "CoFeBX layers for MgO-based magnetic tunnel junction sensors with improved magnetoresistance and noise performance," AIP Adv. **13**(2), 025108 (2023).
[4]P. D. Kulkarni, H. Iwasaki, and T. Nakatani, "The effect of geometrical overlap between giant magnetoresistance sensor and magnetic flux concentrators: A novel comb-shaped sensor for improved sensitivity," Sensors **22**(23), 9385 (2022).
[5]M. Oogane, K. Fujiwara, A. Kanno, T. Nakano, H. Wagatsuma, T. Arimoto, S. Mizukami, S. Kumagai, H. Matsuzaki, N. Nakasato, and Y. Ando, "Sub-pT magnetic field detection by tunnel magneto-resistive sensors," Appl. Phys. Express **14**(12), 123002 (2021).
[6]E. Paz, R. Ferreira, and P. P. Freitas, "Linearization of magnetic sensors with a weakly pinned free-layer MTJ stack using a three-step annealing process," IEEE Trans. Magn. **52**(7), 1–4 (2016).
[7]A. Bocheux, C. Cavoit, M. Mouchel, C. Ducruet, R. Fons, P. Sabon, I.-L. Prejbeanu, and C. Baraduc, in *2016 IEEE Sensors Applications Symposium (SAS)* (IEEE, 2016), pp. 1–5.
[8]T. Nakatani, H. Suto, P. D. Kulkarni, H. Iwasaki, and Y. Sakuraba, "Tunnel magnetoresistance sensors with symmetric resistance-field response and noise properties under AC magnetic field modulation," Appl. Phys. Lett. **121**(19), 192406 (2022).
[9]S. Shirotori, A. Kikitsu, Y. Higashi, Y. Kurosaki, and H. Iwasaki, "Symmetric response magnetoresistance sensor with low 1/f noise by using an antiphase AC modulation bridge," IEEE Trans. Magn. **57**(2), 1–5 (2021).
[10]R. Ferreira, E. Paz, P. P. Freitas, J. Wang, and S. Xue, "large area and low aspect ratio linear magnetic tunnel junctions with a soft-pinned sensing layer," IEEE Trans. Magn. **48**(11), 3719–3722 (2012).
[11]B. Negulescu, D. Lacour, F. Montaigne, A. Gerken, J. Paul, V. Spetter, J. Marien, C. Duret, and M. Hehn, "Wide range and tunable linear magnetic tunnel junction sensor using two exchange pinned electrodes," Appl. Phys. Lett. **95**(11), 112502 (2009).
[12]J. Y. Chen, J. F. Feng, and J. M. D. Coey, "Tunable linear magnetoresistance in MgO magnetic tunnel junction sensors using two pinned CoFeB electrodes," Appl. Phys. Lett. **100**(14), 142407 (2012).
[13]A. Aharoni, "Demagnetizing factors for rectangular ferromagnetic prisms," J. Appl. Phys. **83**(6), 3432–3434 (1998).
[14]M. Beleggia, M. D. Graef, Y. T. Millev, D. A. Goode, and G. Rowlands, "Demagnetization factors for elliptic cylinders," J. Phys. D **38**(18), 3333 (2005).
[15]S. Cardoso, D. C. Leitao, L. Gameiro, F. Cardoso, R. Ferreira, E. Paz, and P. P. Freitas, "Magnetic tunnel junction sensors with pTesla sensitivity," Microsyst. Technol. **20**(4–5), 793–802 (2014).
[16]J. Hu, M. Ji, W. Qiu, L. Pan, P. Li, J. Peng, Y. Hu, H. Liu, and M. Pan, "Double-gap magnetic flux concentrator design for high-sensitivity magnetic tunnel junction sensors," Sensors **19**(20), 4475 (2019).
[17]Z. Marinho, S. Cardoso, R. Chaves, R. Ferreira, L. V. Melo, and P. P. Freitas, "Three dimensional magnetic flux concentrators with improved efficiency for magnetoresistive sensors," J. Appl. Phys. **109**(7), 07E521 (2011).
[18]G. He, Y. Zhang, L. Qian, G. Xiao, Q. Zhang, J. C. Santamarina, T. W. Patzek, and X. Zhang, "PicoTesla magnetic tunneling junction sensors integrated with double staged magnetic flux concentrators," Appl. Phys. Lett. **113**(24), 242401 (2018).
[19]J. Valadeiro, D. C. Leitao, S. Cardoso, and P. P. Freitas, "Improved efficiency of tapered magnetic flux concentrators with double-layer architecture," IEEE Trans. Magn. **53**(11), 1–5 (2017).
[20]J.-M. Quemper, S. Nicolas, J. P. Gilles, J. P. Grandchamp, A. Bosseboeuf, T. Bourouina, and E. Dufour-Gergam, "Permalloy electroplating through photoresist molds," Sens. Actuators A **74**(1), 1–4 (1999).
[21]N. Saito, H. Fujiwara, and Y. Sugita, "A new type of magnetic domain structure in negative magnetostriction Ni-Fe films," J. Phys. Soc. Jpn. **19**(7), 1116–1125 (1964).
[22]P. Zou, W. Yu, and J. A. Bain, "Influence of stress and texture on soft magnetic properties of thin films," IEEE Trans. Magn. **38**(5), 3501–3520 (2002).